Favored α-decay half-lives of odd-A and odd-odd nuclei using an improved density-dependent cluster model with anisotropic surface diffuseness

Zhen Wang [1,*] and Zhongzhou Ren[1,2,†]

[1]*School of Physics Science and Engineering, Tongji University, Shanghai 200092, China*
[2]*Key Laboratory of Advanced Micro-Structure Materials, Ministry of Education, Shanghai 200092, China*

We extend the improved density-dependent cluster model (DDCM+) of our recent work [Wang *et al.*, Phys. Rev. C **105**, 024327 (2022)] to study the favored α decays of odd-A and odd-odd nuclei with $Z \geqslant 82$. In this work, the effective α-core interactions are determined using the double-folding potential with a realistic M3Y-Reid nucleon-nucleon interaction plus proton-proton Coulomb interaction, in which a deformation-dependent diffuseness correction is validated to address the surface anisotropy and polarization effects in nucleon density distribution. It is found that calculations within the anisotropic diffuseness would yield longer calculated α decay half-lives and suggest larger estimated α-preformation factors, which is quite consistent with the conclusions obtained for the even-even α emitters. Meanwhile, the theoretical half-lives agree very well with the experimental data for the favored α decays of the odd-A and odd-odd nuclei with a mean factor of 1.94 and 1.61, respectively. Remarkably, the experimental α-decay half-life of the new thorium isotope ^{207}Th [Yang *et al.*, Phys. Rev. C **105**, L051302 (2022)] is also well reproduced with a factor of about 2.50. Furthermore, we present the quantitative predictions on the favored α-decay half-lives of ^{293,294}119 and ^{294,295}120 α-decay chains in this work, which are expected to serve as useful references for the synthesis of new isotopes in the future.

I. INTRODUCTION

Exploring the nuclear landscape is of high priority in modern nuclear physics. To date, with the advances in radioactive ion beam facilities and detection technologies, many nuclides up to $Z = 118$ (oganesson, Og) have been synthesized via the cold, warm, or hot fusion reactions in the laboratory [1–4]. Nonetheless, the synthesis of nuclides with $Z \geqslant 119$ and the explorations of the nuclear landscape boundaries remain exceedingly challenging tasks [2,5], necessitating further studies on the stability and decay properties of nuclei. α decay is one of the dominant decay channels for unstable nuclei, as the emitted α particles are ideal observations to be easily and accurately detected in experiments, it provides a powerful tool to probe the nuclear structure and simultaneously identify the new elements or nuclides via observing α decays from the parent nucleus to their descendants [2–8]. Therefore, more accurate and reliable theoretical models or methods of α decay are required for the further synthesis of new nuclides.

Theoretically, α decay can be interpreted as the quantum tunneling process of a preformed α cluster near the nuclear surface [9–12]. Due to the complexity of the nuclear many-body problem, the α emitter is often assumed to be a binary system of an α cluster interacting with the remaining core (daughter) nucleus in the most of phenomenological models, see, e.g., Refs. [12–24] and the papers cited therein, for comprehensive reviews. Effective interactions between

α cluster and core nucleus are extremely crucial inputs to study α decay, no matter which theoretical model we adopt. To gain the reliable α-core interaction potentials, the precise description of the nucleon density distribution is necessary in addition to the effective nucleus-nucleus interactions [25,26]. As we all know, nuclear diffuseness plays an important role in determining the nuclear density profiles and interaction potential, one can get the insight that any exotic property of nuclear diffuseness would have a significant impact on the α decay process. Over the past years, the nuclear surface diffuseness is usually presented to be isotropic, though the various types of diffuseness are used in the α-decay calculations [15,16,27]. Very recently, motivated by the works of Refs. [28–30], we have proposed an improved version of the density-dependent cluster model DDCM+ by absorbing the anisotropic nuclear surface diffuseness into the α-decay calculations, and have attempted to explore the effects of nuclear diffuseness anisotropy and polarization on α decay for even-even α emitters [31]. It has been found that the DDCM+ brings in a significant improvement in the agreements between the theoretical half-lives and experimental data for a wide range of even-even nuclei in contrast to the conventional density-dependent cluster model [31].

In this work, we make a further extension of the DDCM+ to investigate the α-decay properties for odd-A and odd-odd nuclei. Here, we consider those α decays with the same spins and parities in initial and final states, in which the orbital angular momentum carried by α cluster vanishes, called favored α decays [32]. A systematic calculation has been performed for the favored α-decay half-lives of the nuclei with a wide range of $Z \geqslant 82$, including the newly reported thorium

---

*wang_zhen@tongji.edu.cn
†Corresponding author: zren@tongji.edu.cn

isotope ^{207}Th [33]. The present study is a natural generalization of our recent work in Ref. [31], and concurrently a test of the validity of DDCM+ for the odd-A and odd-odd nuclei as well. In addition, the synthesis of superheavy nuclei has attracted much attention in recent years. we also expect to give some valuable predictions on the α decay half-lives of unknown nuclides by using the DDCM+. The related numerical results would be analyzed and discussed in detail in Sec. III.

The remaining parts of this paper are organized as follows. The theoretical framework of DDCM+ together with the deformation-dependent anisotropic diffuseness correction are presented in detail in Sec. II. In Sec. III, we first present the numerical results of α decay half-lives for observed odd-A and odd-odd nuclei with $Z \geqslant 82$. Then we continue to give the quantitative predictions on the α decay half-lives of ^{293,294}119 and ^{294,295}120 α-decay chains, which may be beneficial in the future for the synthesis and identification of these undiscovered nuclides. Finally, a summary is given in Sec. IV.

II. THEORETICAL FRAMEWORK

In the present work, the α-decay calculations are performed in the improved density-dependent cluster model DDCM+ [31]. The α-emitter under investigation is assumed to be a binary system of a spherical α cluster interacting with an axially symmetric deformed core nucleus. According to the double-folding models [34], we can respectively calculate the nuclear and Coulomb interactions as

$$V_N(r, \xi) = \lambda(\xi) \int d\mathbf{r}_\alpha \int d\mathbf{r}_c \left[\rho_\alpha^p(\mathbf{r}_\alpha) + \rho_\alpha^n(\mathbf{r}_\alpha) \right]$$
$$\times \left[\rho_c^p(\mathbf{r}_c) + \rho_c^n(\mathbf{r}_c) \right] v(s = |\mathbf{r}_c + \mathbf{r} - \mathbf{r}_\alpha|) \quad (1)$$

and

$$V_C(r, \xi) = \frac{1}{4\pi\varepsilon_0} \int d\mathbf{r}_\alpha \int d\mathbf{r}_c \frac{e^2}{s = |\mathbf{r}_c + \mathbf{r} - \mathbf{r}_\alpha|}$$
$$\times \rho_\alpha^p(\mathbf{r}_\alpha) \rho_c^p(\mathbf{r}_c). \quad (2)$$

In Eqs. (1) and (2), ξ is the orientation angle, $\lambda(\xi)$ is the strength factor of the nuclear potential depth. Instead of a uniform value over the all orientation angles [15,16], the specific value of $\lambda(\xi)$ is determined separately at each angle by reproducing the α-decay energy Q_α for the quasibound state in subsequent calculations. $\rho_\alpha^{p,n}(\mathbf{r}_\alpha)$ and $\rho_c^{p,n}(\mathbf{r}_c)$ denote the proton (denoted by p) and neutron (denoted by n) density distribution for the α cluster and core nucleus, respectively. $s = |\mathbf{r}_c + \mathbf{r} - \mathbf{r}_\alpha|$ is the relative separation between the two interacting nucleons in the α-core system, while the strength of M3Y-Reid nucleon-nucleon interaction $v(s)$ is given as [35]

$$v(s) = 7999.00 \frac{\exp(-4s)}{4s} - 2134.25 \frac{\exp(-2.5s)}{2.5s}$$
$$+ \hat{J}_{00}(E_\alpha) \delta(s). \quad (3)$$

To account for the effect of antisymmetrization due to the single-particle knock-on exchange between two interactive nucleons, a simple energy-dependent zero-range pseudopotential is adopted [36]:

$$\hat{J}_{00}(E_\alpha) = -276 \left[1 - 0.005 \left(\frac{E_\alpha}{A_\alpha} \right) \right], \quad (4)$$

where E_α/A_α represents the kinetic energy per nucleon of the emitted α cluster.

The proton and neutron density distribution for the spherical α cluster are taken to be the standard Gaussian form $\rho_\alpha^\tau(\mathbf{r}_\alpha) = \rho_\alpha^{\tau_0} \exp(-0.7024|\mathbf{r}_\alpha|^2)$ with $\tau_{(0)} = p_{(0)}$ or $n_{(0)}$. As for the core nucleus, the density distribution of the protons and neutrons are described by the two-parameter Fermi (2pF) form

$$\rho_c^\tau(\mathbf{r}_c) = \frac{\rho_c^{\tau_0}}{1 + \exp\left[\frac{|\mathbf{r}_c| - R^\tau(\theta)}{a^\tau(\theta)} \right]} \quad (5)$$

with the half-radius parameter

$$R^\tau(\theta) = R_0^\tau \left[1 + \sum_{i=2,4,6} \beta_i Y_{i0}(\theta) \right]. \quad (6)$$

β_i ($i = 2, 4, 6$) in Eq. (6) represent the multipole deformation parameters. In the DDCM+, we take the surface anisotropy and polarization effects into account by replacing the isotropic diffuseness parameter with the anisotropic one as

$$a^\tau(\theta) = a_\perp^\tau(\theta) \sqrt{1 + \left[\frac{1}{R^\tau(\theta)} \frac{dR^\tau(\theta)}{d\theta} \right]^2}, \quad (7)$$

in which $a_\perp^\tau(\theta) = a_\perp^{\tau_0}[1 - \beta_2 Y_{20}(\theta)]$, and $a_\perp^{\tau_0}$ is determined by $\int_0^{\frac{\pi}{2}} a^\tau(\theta) \sin(\theta) d\theta = a_0^\tau$. Here, we refer to Refs. [28,29,31] for more details. Furthermore, for a core nucleus with proton number Z_c and neutron number N_c, the values of R_0^τ and a_0^τ are estimated in present work by the São Paulo parametrization with [37]

$$R_0^p = 1.81 Z_c^{1/3} - 1.12 \,\text{fm}, \quad a_0^p = 0.47 - 0.00083 Z_c \,\text{fm},$$
$$R_0^n = 1.49 N_c^{1/3} - 0.79 \,\text{fm}, \quad a_0^n = 0.47 - 0.00046 N_c \,\text{fm}, \quad (8)$$

respectively, which consider the difference between proton and neutron density distribution.

Within the theoretical framework of the model DDCM+, the orientation-dependent partial α-decay widths are determined using the distorted wave approach [26,38]

$$\Gamma(\xi) = \frac{4\mu}{\hbar^2 k} \left| \int_0^\infty F_L(kr) [V_N(r, \xi) + \delta V_C(r, \xi)] \varphi_L(r, \xi) \, dr \right|^2, \quad (9)$$

where $\delta V_C(r, \xi) = V_C(r, \xi) - Z_\alpha Z_c e^2/(4\pi\varepsilon_0 r)$. $F_L(kr)$ is the regular Coulomb wave function with $k = \sqrt{2\mu Q_\alpha}/\hbar$, and $\varphi_L(r, \xi)$ is the radial wave function for each certain orientation angle. The internal nodes in the radial wave function are determined by the well-known Wildermuth-Tang condition $G = 2n + L$ [39], which approximately account for the Pauli-blocking effect. Here, the global quantum number G is taken as $G = 22$ for $N > 126$ and $G = 20$ for $82 < N \leqslant 126$. Subsequently, The total α-decay width thus can be obtained
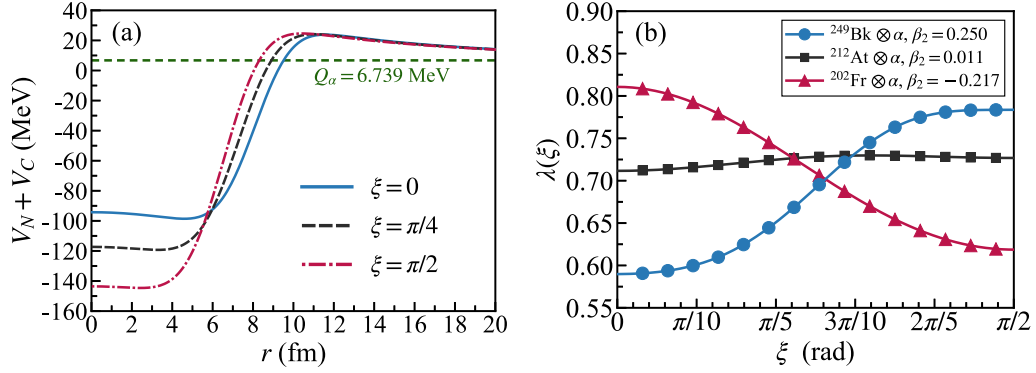
FIG. 1. (a) The sum of nuclear and Coulomb potential versus the distance between the center of mass of the α cluster and core nucleus for the α decay of ^{253}Es $\rightarrow$ ^{249}Bk $+\alpha$. The blue solid line, black dashed line, and red dot-dash line denote the total interactions at three orientation angles $\xi = 0$, $\pi/4$, and $\pi/2$, respectively. The green dashed line at 6.739 MeV denotes the α-decay energy of ^{253}Es. (b) The strength factor $\lambda(\xi)$ of double-folding nuclear potential varies with the orientation angles for the systems of ^{249}Bk $\otimes\alpha$ (blue circles), ^{212}At $\otimes\alpha$ (black squares), and ^{202}Fr $\otimes\alpha$ (red triangles), respectively.

by averaging the partial decay width over the different orientations as [16,18]

$$\Gamma = \int_0^{\frac{\pi}{2}} \Gamma(\xi) \sin\xi \, d\xi. \qquad (10)$$

Finally, the α-decay half-life T_α reads

$$T_\alpha = \frac{\hbar \ln 2}{P_\alpha \Gamma}, \qquad (11)$$

where P_α denotes the preformation probability of the α cluster in parent nucleus. Considering the fact that the P_α factor has a value less than unity and varies smoothly in the open-shell region [12], in present work, we take different constant values for the preformation factor P_α of the odd-A and odd-odd nuclei respectively, to minimize the number of free parameters.

III. NUMERICAL RESULTS AND DISCUSSIONS

In this section, we extend the DDCM+ introduced in Sec. II to study the favored α decays of odd-A and odd-odd nuclei. Before presenting the theoretical results of the α-decay calculations, we reexamine the impacts of the surface diffuseness anisotropy on the α-decay dynamics for the odd-A and odd-odd nuclei, testing the validity and consistency of the conclusions drawn from the even-even α-emitters in our previous work of Ref. [31]. We first concentrate our attention on the influences of the anisotropic surface diffuseness on the effective α-core interaction potentials.

In Fig. 1(a), we illustrate the sum of nuclear and Coulomb potential between the α cluster and deformed ^{249}Bk core nucleus at three different orientation angles $\xi = 0$, $\pi/4$, and $\pi/2$, in which the multipole deformation parameters β_i ($i = 2, 4, 6$) are derived from FRDM2012 [40]. As shown in Fig. 1(a), the deformation can change the barrier height and well depth at different orientations. The total potential at $\xi = 0$ is more attractive than those at the other orientations in the surface region, implying that there is a large overlap between the nuclear density distribution of α cluster and core nucleus at the orientation angle $\xi = 0$.

We continue to plot the strength factor $\lambda(\xi)$ varying with the orientation angles in Fig. 1(b), for the systems of ^{249}Bk $\otimes\alpha$, ^{212}At $\otimes\alpha$, and ^{202}Fr $\otimes\alpha$, respectively. As can be seen, the parameter $\lambda(\xi)$ has a value smaller than one and depends strongly on the orientation angles ξ as well as the values of deformation parameters β_i. Additionally, the value of $\lambda(\xi)$ increases with the orientation angle for the nuclei with positive β_2 whereas conversely with the negative one. The variation of the $\lambda(\xi)$ with the orientation angle suggests that it would be better if the $\lambda(\xi)$ is determined separately at each angle ξ, especially for the well-deformed nuclei. Furthermore, it is of great interest to have a look at how the strength factor varies with the different nuclei. For simplicity, we plot the average strength factor $\langle\lambda\rangle$ over the all angles versus the mass number A_d of the daughter nuclei in Fig. 2, where the value of
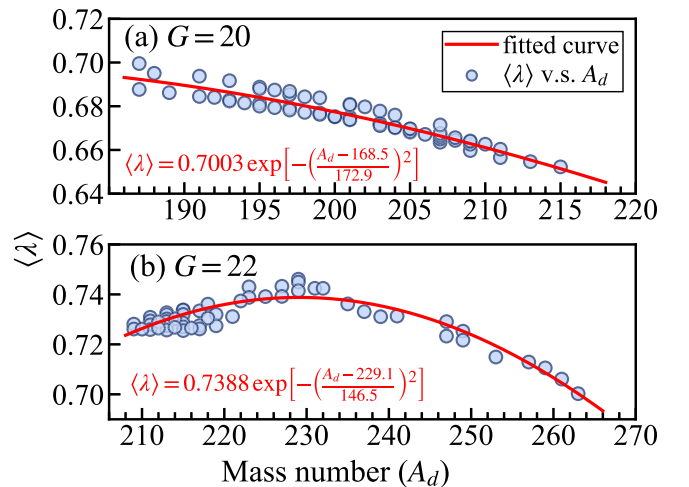

FIG. 2. The average strength factor $\langle\lambda\rangle$ over the all orientation angles versus the mass number of daughter nuclei with the choices of (a) $G = 20$ and (b) $G = 22$, respectively. Note the Gaussian-like fitted curves in red are to guide the eyes.
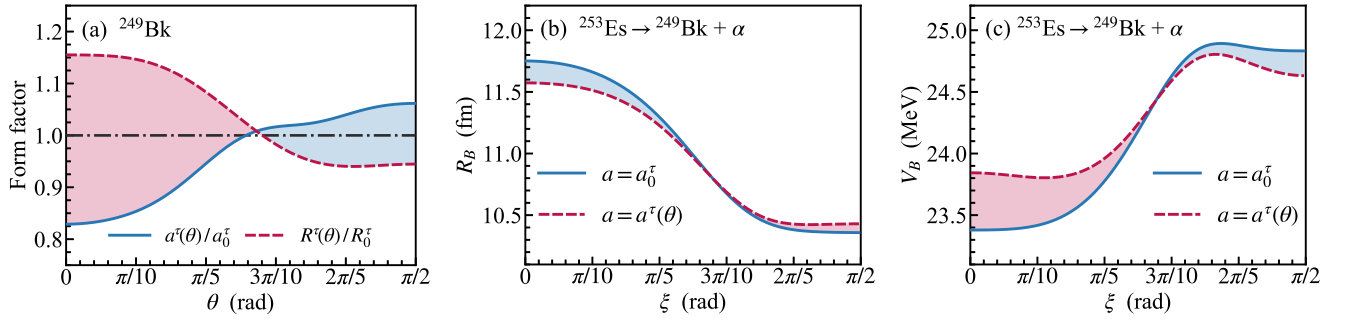
FIG. 3. (a) The form factors of anisotropic diffuseness $a^\tau(\theta)/a_0^\tau$ (blue solid line) and half-density radius $R^\tau(\theta)/R_0^\tau$ (red dashed line) as a function of angle θ for ^{249}Bk. (b) The position and (c) the height of α-core effective potential barrier versus the orientation angle ξ for the decay channel ^{253}Es $\rightarrow$ ^{249}Bk $+\alpha$. The theoretical results calculated with the isotropic diffuseness a_0^τ are denoted by the blue solid lines, while ones calculated with anisotropic diffuseness $a^\tau(\theta)$ are denoted by the red dashed lines in each panel.

$\langle\lambda\rangle$ is obtained by

$$\langle\lambda\rangle = \int_0^{\frac{\pi}{2}} \lambda(\xi)\sin\xi \, d\xi. \tag{12}$$

In Fig. 2, the $\langle\lambda\rangle$ values are divided into two parts, each with a different value of G being adopted. As demonstrated, a larger value of G actually yields a larger $\langle\lambda\rangle$. Moreover, an exponential decay pattern of the $\langle\lambda\rangle$ values is discovered in each panel of Fig. 2, which stimulates us to tentatively propose a Gaussian-like formula to describe the dependence of $\langle\lambda\rangle$ on the mass number A_d. The fitted formulas and corresponding curves are displayed in Figs. 2(a) and 2(b), respectively. From Figs. 2(a) and 2(b), we can see that the red fitted curves fit the data very well. Nevertheless, it is worth noting that the current study is just a preliminary exploration on the behavior of the $\langle\lambda\rangle$ for odd-A and odd-odd α emitters. Some important features of the systematic behavior of the $\langle\lambda\rangle$ are not yet well described since only partial nuclei are considered in the present work. For example, according to the saturation property of the nucleus from the perspective of the liquid drop model, the value of $\langle\lambda\rangle$ should approach asymptotically to a specific value at the large mass number. This asymptotic value, however, can not be well determined in this work since a flat trend does not appear in Fig. 2 with the present data. Simultaneously, the dependence of $\langle\lambda\rangle$ on the proton number is also requested to be determined. A more comprehensive study on the behavior of $\langle\lambda\rangle$ can be anticipated by involving more data in future works, which may provide valuable information on the fundamental properties of the unknown α emitters, such as the effective α-core potential, α-decay energy, and α-decay half-lives, etc., in a novel way [41].

Figure 3(a) shows the form factors of diffuseness $a^\tau(\theta)/a_0^\tau$ (blue solid line) and half-density radius $R^\tau(\theta)/R_0^\tau$ (red dashed line) parameters varying with the angle θ for the daughter nuclei ^{249}Bk. The black dot-dash line corresponds to the isotropic diffuseness and radius parameters of spherical case. One can get the insight from Fig. 3(a), due to the deformation, the diffuseness and radius parameters become to be anisotropic, and the diffuseness tends to reduce along the elongated axis while increasing along the compressed axis, which is known as the polarization of the nuclear surface diffuseness [29]. Consistent with the double-folding poten-

tial in Eqs. (1) and (2), the non-negligible fluctuation of the diffuseness is anticipated to influence the properties of the effective α-core interactions. Here, we still take the α decay of ^{253}Es $\rightarrow$ ^{249}Bk $+\alpha$ for an instance, and the illustrations of the effects of diffuseness anisotropy on the effective α-core interactions are present in Figs. 3(b) and 3(c).

Figures 3(b) and 3(c) plots the the position R_B and height V_B of the potential barrier of ^{249}Bk $\otimes\alpha$ system as a function of the orientation angle ξ, which are respectively calculated with a_0^τ (blue solid lines) and $a^\tau(\theta)$ (red dashed lines). We see in Figs. 3(b) and 3(c) that the diffuseness anisotropy and polarization can induce an increase or decrease of the potential well width and the barrier height. As shown, for the system of ^{249}Bk $\otimes\alpha$, the anisotropic diffuseness brings in a narrower potential well and a higher barrier at small orientation angle ξ, whereas the situation reverses for larger orientation angles. Since the penetration probability of the α cluster is extremely sensitive to the height of the inner potential barrier, the exterior wave function tends to have a significant variation due to the change of the barrier height and will ultimately modify the theoretical α-decay half-lives. Then, without considering the α-preformation factor P_α temporarily, the DDCM+ gives the theoretical half-life of 1.12×10^5 s with anisotropic diffuseness $a^\tau(\theta)$, while 9.11×10^4 s with isotropic one, implying the diffuseness anisotropy conducts to an increase of about 22.9% in the α-decay half-life of ^{253}Es. Furthermore, throughout the global calculations, the changes of α-decay half-lives due to diffuseness anisotropy are found to be much more significant in the nuclei with larger deformation parameters while they are not evident in nuclei with minor ones. This can be easily understood. As discussed in Ref. [31], the diffuseness anisotropy depends on the nuclear deformation degree. It would be much more evident for the diffuseness anisotropy effects as the system become more and more deformed. On the contrary, if the deformation parameters are close to zero, the nuclear profile would be automatically back to the spherical case and the diffuseness would be approximately isotropic, then the impacts of diffuseness anisotropy on α-decay dynamics would be definitely slight in these nuclei.

Next, we investigate the favored α decays of 95 odd-A nuclei and 26 odd-odd nuclei by using the model DDCM+. The favored assumption is true for even-even nuclei. However, the situation is much more complicated for odd-A and

TABLE I. Calculations on the α-decay half-lives of the odd-A and odd-nuclei with $Z \geqslant 82$, from the ground state to ground state. In this table, Q_α denotes the α decay energy taken from Refs. [42,43], β_2, β_4, and β_6 are separately the quadrupole, hexadecapole, and hexacontatetrapole deformation parameters for the daughter nuclei taken from Ref. [40]. T_α^{Exp} denotes the α-decay experimental half-lives, while T_α^{Cal} denotes the theoretical α-decay half-lives given by DDCM+. The experimental half-lives are mainly taken from Ref. [44], while the experimental data comes from the other references are marked in the first column.

α decay	Q_α (MeV)	β_2	β_4	β_6	T_α^{Exp} (s)	T_α^{Cal} (s)
odd-A nuclei, $P_\alpha = 0.0926$						
^{191}Pb $\rightarrow$ ^{187}Hg $+\alpha$ [45]	5.402	−0.146	−0.015	0.003	6.14×10^5	5.65×10^5
^{191}Po $\rightarrow$ ^{187}Pb $+\alpha$	7.493	0.011	0.000	0.000	2.20×10^{-2}	1.43×10^{-2}
^{193}Po $\rightarrow$ ^{189}Pb $+\alpha$	7.094	0.000	0.000	0.000	3.99×10^{-1}	2.95×10^{-1}
^{195}Po $\rightarrow$ ^{191}Pb $+\alpha$	6.750	0.000	0.000	0.000	4.94×10^0	4.99×10^0
^{197}Po $\rightarrow$ ^{193}Pb $+\alpha$	6.411	0.021	0.000	0.000	1.22×10^2	1.01×10^2
^{199}Po $\rightarrow$ ^{195}Pb $+\alpha$	6.074	0.032	0.000	0.000	4.38×10^3	2.64×10^3
^{201}Po $\rightarrow$ ^{197}Pb $+\alpha$	5.799	0.011	0.000	0.000	8.28×10^4	4.68×10^4
^{205}Po $\rightarrow$ ^{201}Pb $+\alpha$	5.325	0.000	0.000	0.000	1.57×10^7	1.12×10^7
^{207}Po $\rightarrow$ ^{203}Pb $+\alpha$	5.216	0.000	0.000	0.000	9.94×10^7	4.18×10^7
^{213}Po $\rightarrow$ ^{209}Pb $+\alpha$	8.536	−0.011	0.000	0.000	3.71×10^{-6}	3.47×10^{-6}
^{215}Po $\rightarrow$ ^{211}Pb $+\alpha$	7.526	0.000	0.000	0.000	1.78×10^{-3}	2.65×10^{-3}
^{217}Po $\rightarrow$ ^{213}Pb $+\alpha$	6.662	0.000	0.000	0.000	1.57×10^0	2.69×10^0
^{219}Po $\rightarrow$ ^{215}Pb $+\alpha$	5.914	0.000	0.000	0.000	2.19×10^3	3.79×10^3
^{197}At $\rightarrow$ ^{193}Bi $+\alpha$	7.104	0.075	0.014	0.001	4.04×10^{-1}	6.06×10^{-1}
^{199}At $\rightarrow$ ^{195}Bi $+\alpha$	6.777	−0.052	0.013	−0.001	7.89×10^0	9.29×10^0
^{201}At $\rightarrow$ ^{197}Bi $+\alpha$	6.473	−0.052	0.013	−0.001	1.20×10^2	1.39×10^2
^{203}At $\rightarrow$ ^{199}Bi $+\alpha$	6.210	−0.052	0.013	−0.001	1.43×10^3	1.69×10^3
^{205}At $\rightarrow$ ^{201}Bi $+\alpha$	6.020	−0.052	0.013	−0.001	1.61×10^4	1.12×10^4
^{207}At $\rightarrow$ ^{203}Bi $+\alpha$	5.873	−0.042	0.001	0.000	6.52×10^4	5.15×10^4
^{209}At $\rightarrow$ ^{205}Bi $+\alpha$	5.757	−0.042	0.001	0.000	5.00×10^5	1.73×10^5
^{211}At $\rightarrow$ ^{207}Bi $+\alpha$	5.982	−0.021	0.000	0.000	6.21×10^4	1.33×10^4
^{213}At $\rightarrow$ ^{209}Bi $+\alpha$	9.254	−0.011	0.000	0.000	1.25×10^{-7}	1.37×10^{-7}
^{215}At $\rightarrow$ ^{211}Bi $+\alpha$	8.178	−0.010	0.012	0.000	3.70×10^{-5}	7.34×10^{-5}
^{217}At $\rightarrow$ ^{213}Bi $+\alpha$	7.201	−0.010	0.012	0.000	3.26×10^{-2}	7.86×10^{-2}
^{219}At $\rightarrow$ ^{215}Bi $+\alpha$	6.342	−0.021	0.012	0.000	5.98×10^1	1.45×10^2
^{195}Rn $\rightarrow$ ^{191}Po $+\alpha$	7.694	−0.217	0.017	−0.001	7.00×10^{-3}	1.43×10^{-2}
^{197}Rn $\rightarrow$ ^{193}Po $+\alpha$	7.411	−0.217	0.017	−0.001	5.40×10^{-2}	1.12×10^{-1}
^{199}Rn $\rightarrow$ ^{195}Po $+\alpha$	7.132	−0.207	0.015	−0.001	5.90×10^{-1}	9.87×10^{-1}
^{203}Rn $\rightarrow$ ^{199}Po $+\alpha$	6.630	0.075	0.002	0.000	6.70×10^1	8.44×10^1
^{207}Rn $\rightarrow$ ^{203}Po $+\alpha$	6.251	−0.063	0.001	0.000	2.64×10^3	2.86×10^3
^{209}Rn $\rightarrow$ ^{205}Po $+\alpha$	6.155	−0.052	0.001	0.000	1.02×10^4	7.12×10^3
^{215}Rn $\rightarrow$ ^{211}Po $+\alpha$	8.839	−0.011	0.000	0.000	2.30×10^{-6}	2.98×10^{-6}
^{217}Rn $\rightarrow$ ^{213}Po $+\alpha$	7.887	0.000	0.000	0.000	5.93×10^{-4}	1.21×10^{-3}
^{199}Fr $\rightarrow$ ^{195}At $+\alpha$	7.817	−0.217	0.017	−0.001	6.60×10^{-3}	1.29×10^{-2}
^{201}Fr $\rightarrow$ ^{197}At $+\alpha$	7.519	−0.207	0.015	−0.001	6.28×10^{-2}	1.12×10^{-1}
^{203}Fr $\rightarrow$ ^{199}At $+\alpha$	7.275	0.096	0.003	0.000	5.50×10^{-1}	8.62×10^{-1}
^{205}Fr $\rightarrow$ ^{201}At $+\alpha$	7.055	0.086	−0.009	−0.001	3.96×10^0	5.03×10^0
^{207}Fr $\rightarrow$ ^{203}At $+\alpha$	6.889	−0.083	0.014	0.009	1.56×10^1	1.96×10^1
^{209}Fr $\rightarrow$ ^{205}At $+\alpha$	6.778	−0.073	0.002	0.000	5.67×10^1	4.97×10^1
^{211}Fr $\rightarrow$ ^{207}At $+\alpha$	6.662	−0.053	−0.011	0.001	2.14×10^2	1.34×10^2
^{213}Fr $\rightarrow$ ^{209}At $+\alpha$	6.905	0.011	0.000	0.000	3.43×10^1	1.41×10^1
^{215}Fr $\rightarrow$ ^{211}At $+\alpha$	9.540	0.000	0.000	0.000	9.00×10^{-8}	1.41×10^{-7}
^{217}Fr $\rightarrow$ ^{213}At $+\alpha$	8.469	−0.011	0.000	0.000	2.20×10^{-5}	6.20×10^{-5}
^{219}Fr $\rightarrow$ ^{215}At $+\alpha$	7.449	0.011	0.000	0.000	2.25×10^{-2}	7.44×10^{-2}
^{201}Ra $\rightarrow$ ^{197}Rn $+\alpha$	8.002	−0.227	0.019	−0.002	2.00×10^{-2}	7.86×10^{-3}
^{203}Ra $\rightarrow$ ^{199}Rn $+\alpha$	7.736	−0.217	0.017	−0.001	3.60×10^{-2}	5.08×10^{-2}
^{205}Ra $\rightarrow$ ^{201}Rn $+\alpha$	7.486	−0.207	0.004	0.001	2.20×10^{-1}	3.28×10^{-1}
^{209}Ra $\rightarrow$ ^{205}Rn $+\alpha$	7.143	−0.104	0.016	0.008	4.71×10^0	5.45×10^0
^{211}Ra $\rightarrow$ ^{207}Rn $+\alpha$	7.042	−0.084	0.002	0.000	1.26×10^1	1.23×10^1
^{217}Ra $\rightarrow$ ^{213}Rn $+\alpha$	9.161	−0.010	0.012	0.000	1.95×10^{-6}	2.32×10^{-6}
^{205}Ac $\rightarrow$ ^{201}Fr $+\alpha$ [46]	8.093	−0.217	0.006	0.001	2.00×10^{-2}	9.19×10^{-3}
^{207}Ac $\rightarrow$ ^{203}Fr $+\alpha$	7.845	−0.207	−0.007	0.003	3.10×10^{-2}	5.22×10^{-2}

TABLE I. (*Continued.*)

α decay	Q_α (MeV)	β_2	β_4	β_6	T_α^{Exp} (s)	T_α^{Cal} (s)
^{209}Ac $\rightarrow$ ^{205}Fr $+\alpha$	7.730	-0.125	0.018	0.008	9.40×10^{-2}	1.31×10^{-1}
^{211}Ac $\rightarrow$ ^{207}Fr $+\alpha$	7.568	-0.115	0.017	0.008	2.13×10^{-1}	4.26×10^{-1}
^{213}Ac $\rightarrow$ ^{209}Fr $+\alpha$	7.498	-0.084	0.002	0.000	7.38×10^{-1}	7.10×10^{-1}
^{215}Ac $\rightarrow$ ^{211}Fr $+\alpha$	7.746	0.011	0.000	0.000	1.71×10^{-1}	1.02×10^{-1}
^{217}Ac $\rightarrow$ ^{213}Fr $+\alpha$	9.832	0.000	0.000	0.000	6.90×10^{-8}	1.41×10^{-7}
^{219}Ac $\rightarrow$ ^{215}Fr $+\alpha$	8.827	0.000	0.000	0.000	9.40×10^{-6}	3.56×10^{-5}
^{221}Ac $\rightarrow$ ^{217}Fr $+\alpha$	7.792	0.079	0.054	0.021	5.20×10^{-2}	3.01×10^{-2}
^{227}Ac $\rightarrow$ ^{223}Fr $+\alpha$	5.042	0.132	0.083	0.008	4.98×10^{10}	4.59×10^{10}
^{207}Th $\rightarrow$ ^{203}Ra $+\alpha$ [33]	8.328	-0.217	0.006	0.001	9.70×10^{-3}	4.17×10^{-3}
^{211}Th $\rightarrow$ ^{207}Ra $+\alpha$	7.938	-0.125	0.018	0.008	4.80×10^{-2}	6.63×10^{-2}
^{213}Th $\rightarrow$ ^{209}Ra $+\alpha$	7.837	-0.104	0.004	0.009	1.44×10^{-1}	1.34×10^{-1}
^{219}Th $\rightarrow$ ^{215}Ra $+\alpha$	9.506	-0.021	0.012	0.000	1.02×10^{-6}	1.61×10^{-6}
^{211}Pa $\rightarrow$ ^{207}Ac $+\alpha$	8.481	-0.197	-0.020	0.005	6.00×10^{-3}	3.31×10^{-3}
^{213}Pa $\rightarrow$ ^{209}Ac $+\alpha$	8.384	-0.125	0.018	0.008	7.40×10^{-3}	6.56×10^{-3}
^{215}Pa $\rightarrow$ ^{211}Ac $+\alpha$	8.236	-0.094	0.004	0.009	1.40×10^{-2}	1.77×10^{-2}
^{217}Pa $\rightarrow$ ^{213}Ac $+\alpha$	8.489	-0.063	-0.010	-0.009	3.80×10^{-3}	3.02×10^{-3}
^{219}Pa $\rightarrow$ ^{215}Ac $+\alpha$	10.128	0.000	0.000	0.000	5.60×10^{-8}	1.38×10^{-7}
^{221}Pa $\rightarrow$ ^{217}Ac $+\alpha$	9.248	0.000	0.000	0.000	5.90×10^{-6}	1.46×10^{-5}
^{223}Pa $\rightarrow$ ^{219}Ac $+\alpha$	8.343	0.090	0.055	0.012	5.30×10^{-3}	3.43×10^{-3}
^{227}Pa $\rightarrow$ ^{223}Ac $+\alpha$	6.580	0.133	0.083	0.019	2.70×10^{3}	4.33×10^{3}
^{221}U $\rightarrow$ ^{217}Th $+\alpha$	9.889	-0.021	0.012	0.000	6.60×10^{-7}	9.44×10^{-7}
^{229}U $\rightarrow$ ^{225}Th $+\alpha$	6.476	0.143	0.084	0.009	1.73×10^{4}	3.35×10^{4}
^{233}U $\rightarrow$ ^{229}Th $+\alpha$	4.909	0.184	0.113	0.021	5.02×10^{12}	7.39×10^{12}
^{219}Np $\rightarrow$ ^{215}Pa $+\alpha$	9.208	-0.063	-0.022	-0.008	5.70×10^{-4}	1.68×10^{-4}
^{223}Np $\rightarrow$ ^{219}Pa $+\alpha$	9.650	0.055	0.027	0.005	2.50×10^{-6}	6.82×10^{-6}
^{225}Np $\rightarrow$ ^{221}Pa $+\alpha$ [47]	8.818	0.100	0.056	0.013	3.10×10^{-4}	7.82×10^{-4}
^{233}Np $\rightarrow$ ^{229}Pa $+\alpha$	5.627	0.185	0.126	0.024	3.10×10^{8}	7.89×10^{8}
^{231}Pu $\rightarrow$ ^{227}U $+\alpha$	6.839	0.153	0.085	-0.001	3.97×10^{3}	6.92×10^{3}
^{235}Pu $\rightarrow$ ^{231}U $+\alpha$	5.952	0.195	0.114	0.022	5.42×10^{7}	4.45×10^{7}
^{233}Cm $\rightarrow$ ^{229}Pu $+\alpha$	7.474	0.195	0.114	0.022	1.35×10^{2}	8.58×10^{1}
^{239}Cf $\rightarrow$ ^{235}Cm $+\alpha$	7.764	0.215	0.106	0.001	4.31×10^{1}	4.39×10^{1}
^{245}Cf $\rightarrow$ ^{241}Cm $+\alpha$	7.259	0.237	0.086	-0.024	7.65×10^{3}	3.12×10^{3}
^{241}Es $\rightarrow$ ^{237}Bk $+\alpha$	8.259	0.226	0.095	-0.001	5.10×10^{0}	2.14×10^{0}
^{243}Es $\rightarrow$ ^{239}Bk $+\alpha$	8.072	0.226	0.095	-0.012	3.62×10^{1}	8.68×10^{0}
^{251}Es $\rightarrow$ ^{247}Bk $+\alpha$	6.597	0.249	0.051	-0.032	2.38×10^{7}	5.71×10^{6}
^{253}Es $\rightarrow$ ^{249}Bk $+\alpha$	6.739	0.250	0.039	-0.035	1.77×10^{6}	1.21×10^{6}
^{251}No $\rightarrow$ ^{247}Fm $+\alpha$	8.752	0.249	0.051	-0.032	9.64×10^{-1}	7.02×10^{-1}
^{253}Lr $\rightarrow$ ^{249}Md $+\alpha$	8.918	0.250	0.039	-0.035	7.02×10^{-1}	5.02×10^{-1}
^{257}Lr $\rightarrow$ ^{253}Md $+\alpha$ [48]	9.068	0.251	0.015	-0.040	6.00×10^{-1}	1.59×10^{-1}
^{261}Rf $\rightarrow$ ^{257}No $+\alpha$	8.646	0.240	0.000	-0.033	1.17×10^{1}	7.13×10^{0}
^{263}Sg $\rightarrow$ ^{259}Rf $+\alpha$	9.403	0.242	-0.025	-0.028	1.08×10^{0}	1.87×10^{-1}
^{265}Hs $\rightarrow$ ^{261}Sg $+\alpha$	10.470	0.242	-0.025	-0.028	1.96×10^{-3}	1.22×10^{-3}
^{267}Ds $\rightarrow$ ^{263}Hs $+\alpha$	11.777	0.242	-0.038	-0.021	1.00×10^{-5}	5.38×10^{-6}
odd-odd nuclei, $P_\alpha = 0.0712$						
^{192}At $\rightarrow$ ^{188}Bi $+\alpha$	7.696	-0.196	0.014	-0.001	1.15×10^{-2}	8.74×10^{-3}
^{196}At $\rightarrow$ ^{192}Bi $+\alpha$	7.196	0.085	0.015	0.001	3.87×10^{-1}	3.96×10^{-1}
^{198}At $\rightarrow$ ^{194}Bi $+\alpha$	6.889	0.064	0.014	0.001	4.61×10^{0}	4.82×10^{0}
^{200}At $\rightarrow$ ^{196}Bi $+\alpha$	6.596	0.053	0.013	0.001	8.31×10^{1}	6.13×10^{1}
^{202}At $\rightarrow$ ^{198}Bi $+\alpha$	6.354	-0.052	0.013	-0.001	1.53×10^{3}	5.66×10^{2}
^{204}At $\rightarrow$ ^{200}Bi $+\alpha$	6.070	-0.042	0.012	-0.001	1.44×10^{4}	9.26×10^{3}
^{208}At $\rightarrow$ ^{204}Bi $+\alpha$	5.751	-0.052	0.001	0.000	1.07×10^{6}	2.57×10^{5}
^{214}At $\rightarrow$ ^{210}Bi $+\alpha$	8.988	-0.021	0.012	0.000	5.58×10^{-7}	7.59×10^{-7}
^{216}At $\rightarrow$ ^{212}Bi $+\alpha$	7.950	-0.011	0.000	0.000	3.00×10^{-4}	4.35×10^{-4}
^{200}Fr $\rightarrow$ ^{196}At $+\alpha$	7.622	-0.217	0.017	-0.001	4.75×10^{-2}	7.00×10^{-2}
^{202}Fr $\rightarrow$ ^{198}At $+\alpha$	7.385	-0.207	0.015	-0.001	3.72×10^{-1}	4.10×10^{-1}
^{204}Fr $\rightarrow$ ^{200}At $+\alpha$	7.170	0.096	0.003	0.000	1.82×10^{0}	2.62×10^{0}
^{208}Fr $\rightarrow$ ^{204}At $+\alpha$	6.785	-0.084	0.002	0.000	6.64×10^{1}	6.39×10^{1}
^{210}Fr $\rightarrow$ ^{206}At $+\alpha$	6.671	-0.073	0.002	0.000	2.69×10^{2}	1.70×10^{2}

TABLE I. (*Continued.*)

α decay	Q_α (MeV)	β_2	β_4	β_6	T_α^{Exp} (s)	T_α^{Cal} (s)
^{216}Fr $\rightarrow$ ^{212}At $+\alpha$	9.174	0.011	0.012	0.000	7.00×10^{-7}	1.31×10^{-6}
^{218}Fr $\rightarrow$ ^{214}At $+\alpha$	8.014	-0.010	0.000	0.010	1.40×10^{-3}	1.64×10^{-3}
^{206}Ac $\rightarrow$ ^{202}Fr $+\alpha$	7.958	-0.217	0.006	0.001	2.50×10^{-2}	3.09×10^{-2}
^{208}Ac $\rightarrow$ ^{204}Fr $+\alpha$	7.729	-0.197	-0.009	0.003	9.70×10^{-2}	1.64×10^{-1}
^{212}Ac $\rightarrow$ ^{208}Fr $+\alpha$	7.540	-0.094	0.003	0.000	8.95×10^{-1}	7.09×10^{-1}
^{218}Ac $\rightarrow$ ^{214}Fr $+\alpha$	9.384	-0.010	0.012	0.000	1.00×10^{-6}	1.95×10^{-6}
^{222}Ac $\rightarrow$ ^{218}Fr $+\alpha$	7.137	0.090	0.055	0.012	5.05×10^{0}	7.00×10^{0}
^{212}Pa $\rightarrow$ ^{208}Ac $+\alpha$	8.411	-0.125	0.018	0.008	5.80×10^{-3}	7.66×10^{-3}
^{214}Pa $\rightarrow$ ^{210}Ac $+\alpha$	8.271	-0.115	0.005	0.009	1.70×10^{-2}	1.89×10^{-2}
^{220}Pa $\rightarrow$ ^{216}Ac $+\alpha$	9.704	-0.021	0.012	0.000	8.50×10^{-7}	1.60×10^{-6}
^{226}Pa $\rightarrow$ ^{222}Ac $+\alpha$	6.987	0.122	0.082	0.018	1.46×10^{2}	1.37×10^{2}
^{236}Am $\rightarrow$ ^{232}Np $+\alpha$	6.256	0.206	0.116	0.013	5.40×10^{6}	5.12×10^{6}

odd-odd α-emitters, and the spins and parities of some nuclei are even still unknown in experiments. In Ref. [49], Audi *et al.* pointed out that the α decay of an odd-A or odd-odd nuclide in the region of deformation prefer the favored transition with the same Nilsson model quantum number assignment in the parent and daughter nucleus. Therefore, the favored assumption is adopted for the deformed heavy nuclei as well in this work [49]. We first determine the α-preformation factor P_α by optimizing the calculated half-lives with the experimental data for the odd-A and odd-odd nuclei, respectively. As mentioned in Sec. II, here we simply take the constant α preformation factor for certain kinds of α emitters, to reduce the number of free parameters. Within the framework of DDCM+, the α calculations with anisotropic diffuseness yield the P_α values of 0.0926 for odd-A nuclei and 0.0712 for odd-odd nuclei, whereas the calculations with isotropic diffuseness yield the P_α values of 0.0880 for odd-A nuclei and 0.0689 for odd-odd nuclei. It can be seen that the inclusion of diffuseness anisotropy brings in an increase of the P_α value by roughly 5.2% for odd-A nuclei and 3.3% for odd-odd nuclei, which is consistent with the conclusions obtained for even-even α emitters of our previous work [31].

Combining with the deduced P_α, we present the numerical results of α calculations in Table. I. It is worth pointing out that the nuclei with uncertain α-decay branching ratios are not included in current calculations. In Table. I, the first column represents the α-decay channels. The second column denotes the α-decay energy, the values of which are mainly taken from the AME2020 [42,43]. Columns three to five are the quadrupole, hexadecapole and hexacontatetrapole deformation parameters taken from the FRDM2012 [40], respectively. The last two columns list the α-decay half-lives in the unit of seconds with T_α^{Exp} being the experimental α-decay half-lives mainly taken from the NUBASE2020 [44], and T_α^{Cal} being the theoretical α-decay half-lives given by the DDCM+. For the nuclei with multiple decay channels, T_α^{Exp} listed in Table I are derived by

$$T_\alpha^{\text{Exp}} = T_{1/2}^{\text{Exp}}/\gamma_\alpha \tag{13}$$

with $T_{1/2}^{\text{Exp}}$ being the real experimental half-lives, and γ_α being the corresponding α-decay branching ratios. As can be

seen, the theoretical results are in good agreement with the experimental data though the experimental half-lives vary in a wide range from 5.6×10^{-8} s to 5.02×10^{12} s. Very recently, one new isotope ^{207}Th ($Q_\alpha = 8.328$ MeV, $T_\alpha^{\text{Exp}} = 9.7$ ms) has been reported in Ref. [33]. By combining the new data of ^{207}Th with the existing experimental data, the authors have reported an odd-even staggering (OES) behavior in the α-decay energies of the nuclei with $Z > 82$ and $N < 126$ along both isotopic and isotonic chains. Within the relativistic Hartree-Fock-Bogoliubov and large-scale shell-model calculations, the authors deduced that the OES originates from both pairing correlations and blocking of particular orbitals by unpaired nucleons [33]. The newly synthesized isotope ^{207}Th can be a good object to test the accuracy of the DDCM+. As shown in Table I, the DDCM+ reproduce the latest experimental α-decay half-life of the new isotope ^{207}Th with a factor of about 2.50, demonstrating the good reliability and accuracy of the DDCM+ in this mass region.

To see the agreement between the theoretical results and the experimental data more intuitively, we plot the logarithmic deviations $\delta = \log_{10} T_\alpha^{\text{Cal}} - \log_{10} T_\alpha^{\text{Exp}}$ for odd-A and odd-odd nuclei in Figs. 4(a) and 4(b), respectively. The region between two black dot-dash lines corresponds to the deviations within a factor less than three, and the red star in Fig. 4(a) denotes the δ value of new isotope ^{207}Th. As shown, most of the δ values are situated between two dot-dash lines, implying that the theoretical results given by the DDCM+ agree with the latest experimental data very well. Nevertheless, the relatively larger deviations can be seen for the nuclei near the $N = 126$ closed shell and in the superheavy mass region. The former cases are mainly because the constant P_α is not enough to describe the structure effects, fortunately, this problem can be overcome by including the shell effect, the hindrance of the unpaired nucleon, and so on into the α preformation factors P_α, some related studies can be found in Refs. [50–52]. As for the latter cases, the calculated half-lives are found to be shorter than the experimental half-lives for some superheavy nuclei. It is probably because these α decays belong to the unfavored transitions rather than the favored ones, and the α cluster would carry an orbital angular momentum with $L \neq 0$, resulting in a hindrance for the α-decay process due to the additional centrifugal barrier [32]. For example, the α
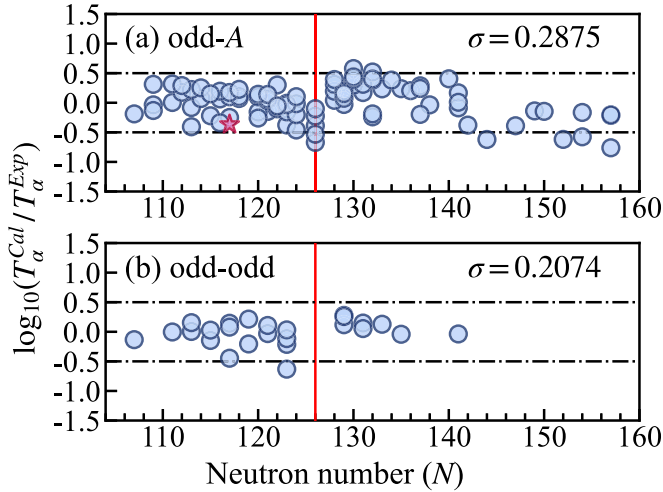
FIG. 4. The logarithmic deviations between the experimental data and the theoretical results given by DDCM+ for (a) odd-A and (b) odd-odd nuclei. The black dot-dash lines in each panel correspond to the deviation between the theoretical results and the experimental data with a factor of three, while the red solid line denotes the neutron number of $N = 126$. The red star in (a) denotes the logarithmic deviation of new isotope ^{207}Th.

decay of ^{263}Sg $\rightarrow$ ^{259}Rf $+\alpha$ is assumed to be favored with the $3/2^+ \rightarrow 3/2^+$ transition in the present calculations, whereas a large logarithmic deviation of $\delta = -0.7612$, corresponding to a factor of 5.77, is obtained under this assumption. Through a further analysis, we assume that the ^{263}Sg may decay from its ground $3/2^+$ state to the low-lying excited $7/2^+$ state of ^{259}Rf with an estimated excitation energy of 60 keV [44], and the α decay of ^{263}Sg should be unfavored with an orbital angular momentum of $L = 2$. With this unfavored assumption, the theoretical α-decay half-life is given by 4.56×10^{-1} s, whose logarithmic deviation reduces to $\delta = -0.3744$, corresponding to a factor of 2.37. As can be seen, the theoretical result has been significantly improved. Consequently, the more abundant information on the α-decay spectrum and nuclear structure in the future would be beneficial to improve the accuracy of these theoretical models.

Furthermore, to have a systematic evaluation on the accuracy of the DDCM+, we calculate the root-mean-square (rms) deviation

$$\sigma = \sqrt{\frac{1}{N_T} \sum_{i=1}^{N_T} \left(\log_{10} T_\alpha^{\text{Cal}, i} - \log_{10} T_\alpha^{\text{Exp}, i} \right)^2} \quad (14)$$

TABLE II. Comparison of the rms deviations between the calculations and the experimental data for odd-A and odd-odd nuclei by using the generalized liquid drop model (GLDM) [53], the improved effective liquid drop model (IMELDM) [54], the generalized density-dependent cluster model (GDDCM) [26], and the DDCM+ model.

	GLDM	IMELDM	GDDCM	DDCM+
odd-A	0.3260	0.8165	0.3460	0.2875
odd-odd	0.2660	0.6785	—	0.2074

TABLE III. Theoretical predictions of α-decay half-lives for the α-decay chains of ^{293,294}119 and ^{294,295}120. In this table, Q_α^{th1} and Q_α^{th2} represent the theoretical α-decay energies calculated by the empirical formula of Ref. [55], and FRDM2012 [40], respectively. T_α^{th1} and T_α^{th2} are the corresponding theoretical α-decay half-lives calculated by using the DDCM+ [31].

Nuclei	Q_α^{th1} (MeV)	T_α^{th1} (s)	Q_α^{th2} (MeV)	T_α^{th2} (s)
the α-decay chain of ^{295}120				
^{295}120	12.574	7.29×10^{-5}	13.460	1.31×10^{-6}
^{291}Og	12.047	2.77×10^{-4}	12.550	2.38×10^{-5}
^{287}Lv	11.639	6.25×10^{-4}	11.200	6.69×10^{-3}
^{283}Fl	11.319	6.76×10^{-4}	9.830	5.17×10^{0}
^{279}Cn	10.988	8.61×10^{-4}	11.650	2.67×10^{-5}
^{275}Ds	10.521	3.09×10^{-3}	10.780	7.12×10^{-4}
^{271}Hs	9.860	3.86×10^{-2}	8.850	3.95×10^{1}
^{267}Sg	9.073	1.61×10^{0}	7.930	1.25×10^{4}
^{263}Rf	8.306	9.14×10^{1}	7.710	1.37×10^{4}
the α-decay chain of ^{294}120				
^{294}120	12.714	2.32×10^{-5}	13.490	7.15×10^{-7}
^{290}Og	12.251	6.27×10^{-5}	12.670	8.47×10^{-6}
^{286}Lv	11.902	1.07×10^{-4}	11.680	3.35×10^{-4}
^{282}Fl	11.599	9.30×10^{-5}	9.960	1.30×10^{0}
^{278}Cn	11.220	1.56×10^{-4}	12.170	1.38×10^{-6}
^{274}Ds	10.662	8.55×10^{-4}	10.380	4.38×10^{-3}
^{270}Hs	9.929	1.59×10^{-2}	8.790	3.93×10^{1}
^{266}Sg	9.142	6.31×10^{-1}	8.120	1.56×10^{3}
^{262}Rf	8.432	2.17×10^{1}	8.100	3.07×10^{2}
the α-decay chain of ^{294}119				
^{294}119	12.154	3.82×10^{-4}	12.850	1.35×10^{-5}
^{290}Ts	11.622	1.63×10^{-3}	11.850	4.97×10^{-4}
^{286}Mc	11.207	4.07×10^{-3}	10.210	1.53×10^{0}
^{282}Nh	10.882	3.80×10^{-2}	10.020	7.23×10^{0}
^{278}Rg	10.544	6.66×10^{-3}	11.260	1.28×10^{-4}
^{274}Mt	10.070	2.72×10^{-2}	10.010	3.95×10^{-2}
^{270}Bh	9.402	4.00×10^{0}	8.330	1.18×10^{4}
^{266}Db	8.608	2.68×10^{1}	7.450	4.99×10^{5}
^{262}Lr	7.833	2.39×10^{3}	7.390	1.30×10^{5}
the α-decay chain of ^{293}119				
^{293}119	12.297	1.51×10^{-4}	12.920	7.88×10^{-6}
^{289}Ts	11.828	4.49×10^{-4}	11.980	2.07×10^{-4}
^{285}Mc	11.472	7.74×10^{-4}	10.300	6.90×10^{-1}
^{281}Nh	11.163	7.19×10^{-4}	10.760	6.84×10^{-3}
^{277}Rg	10.778	1.43×10^{-3}	11.490	3.20×10^{-5}
^{273}Mt	10.214	9.10×10^{-3}	9.780	1.35×10^{-1}
^{269}Bh	9.473	2.22×10^{-1}	8.240	2.09×10^{3}
^{265}Db	8.679	1.25×10^{1}	7.700	3.90×10^{4}
^{261}Lr	7.962	6.28×10^{2}	7.720	5.02×10^{3}

as well. The rms deviations for the odd-A and odd-odd nuclei are 0.2875 and 0.2074, respectively, which means the DDCM+ reproduce the experimental data with average factors of about 1.94 for odd-A nuclei, and 1.61 for odd-odd nuclei. For comparison, the rms deviations for the odd-A and odd-odd nuclei with different models are listed in Table II. These results demonstrate that the DDCM+ is a reliable model in the studies of α-decay half-lives. It is also expected that the DDCM+ can be extended to study the properties of unfavored α decays in the future.

In recent years, the hunt for new elements or nuclides with proton numbers $Z \geqslant 119$ intensifies [5]. α decay, as one of the dominant decay modes for superheavy nuclei, reflects the stability of superheavy nuclei and represents the experimental signatures for their identification [1,5]. Very recently, the fusion reactions ^{54}Cr + ^{243}Am and ^{55}Mn + ^{243}Am with evaporating three or four neutrons are tentatively suggested to reproduce the new elements with $Z = 119$ and 120 [56]. Before the formal experiments, the quantitative predictions on the α-decay properties are required. In view of the reliability of the DDCM+, we continue to make theoretical predictions for the α-decay chains of ^{293,294}119 and ^{294,295}120 isotopes within the framework of DDCM+.

As the crucial inputs of the DDCM+, two versions of α-decay energies Q_α^{th1} and Q_α^{th2}, respectively, calculated from the empirical formula of Ref. [55] and FRDM2012 [40], are used to predict the α-decay half-lives, while the corresponding theoretical α-decay half-lives are denoted by T_α^{th1} and T_α^{th2}, respectively. These theoretical results are listed in Table III. It can be seen that the DDCM+ within these two versions of α-decay energies give different values of theoretical half-lives, especially for ^{267}Sg, ^{270}Hs, and so on, the corresponding theoretical half-lives T_α^{th1} and T_α^{th2} are wildly divergent. This implies that the theoretical half-lives are very sensitive to the α-decay energy. As we all know, the precise predictions on the nuclear mass or α-decay energy are still a pending problem nowadays, therefore, the more precise models or formulas of the nuclear mass are required to improve the accuracy of the α-decay theoretical models in the future. We hope these results could be useful references for future experimental studies on the synthesis of new elements with $Z \geqslant 119$.

IV. SUMMARY

In conclusion, the improved density-dependent cluster model DDCM+ is extended to investigate the favored α decays of the odd-A and odd-odd nuclei with proton numbers $Z \geqslant 82$ in this work. First, we revisit the impacts of surface diffuseness anisotropy and polarization on the α-decay dynamics, and the same conclusions are obtained for the odd-A and odd-odd nuclei with the even-even nuclei. It is found that the anisotropy of nuclear surface diffuseness would lead to a larger estimated α-preformation factor and a longer half-life.

Then, we implement the DDCM+ to study the favored α decays of 95 odd-A and 26 odd-odd nuclei with $Z \geqslant 82$. The theoretical results given by the DDCM+ are in good agreement with the latest experimental data with a mean factor of about 1.94 for odd-A nuclei, and 1.61 for odd-odd nuclei. Noticeably, the theoretical α-decay half-life of new isotope ^{207}Th also agrees well with the experimental data with a factor of 2.50. It demonstrates that the model DDCM+ is indeed a reliable model for the studies of α decay.

For the references of future synthesis of new elements with $Z \geqslant 119$, we also provide the theoretical predictions for the α-decay chains of ^{293,294}119 and ^{294,295}120 isotopes, It is expected that these results could be useful for the forthcoming experimental and theoretical studies on the synthesis of new elements.

[1] Y. Oganessian, J. Phys. G **34**, R165 (2007).

[2] S. A. Giuliani, Z. Matheson, W. Nazarewicz, E. Olsen, P. G. Reinhard, J. Sadhukhan, B. Schuetrumpf, N. Schunck, and P. Schwerdtfeger, Rev. Mod. Phys. **91**, 011001 (2019).

[3] Z. Y. Zhang, H. B. Yang, M. H. Huang, Z. G. Gan *et al.*, Phys. Rev. Lett. **126**, 152502 (2021).

[4] S. Hofmann and G. Munzenberg, Rev. Mod. Phys. **72**, 733 (2000).

[5] A. Såmark-Roth, D. M. Cox, D. Rudolph, L. G. Sarmiento *et al.*, Phys. Rev. Lett. **126**, 032503 (2021).

[6] Z. Ren and B. Zhou, Front. Phys. (Beijing) **13**, 132110 (2018).

[7] M. Ismail and A. Adel, Phys. Rev. C **101**, 024607 (2020).

[8] J. L. Egido and A. Jungclaus, Phys. Rev. Lett. **126**, 192501 (2021).

[9] G. Gamow, Z. Phys. **51**, 204 (1928).

[10] R. W. Gurney and E. U. Condon, Nature (London) **122**, 439 (1928).

[11] K. Varga, R. G. Lovas, and R. J. Liotta, Phys. Rev. Lett. **69**, 37 (1992).

[12] B. Buck, A. C. Merchant, and S. M. Perez, Phys. Rev. C **45**, 2247 (1992).

[13] B. A. Brown, Phys. Rev. C **46**, 811 (1992).

[14] G. Royer, Nucl. Phys. A **848**, 279 (2010).

[15] C. Xu and Z. Ren, Nucl. Phys. A **753**, 174 (2005).

[16] C. Xu and Z. Ren, Phys. Rev. C **74**, 014304 (2006).

[17] P. Mohr, Phys. Rev. C **73**, 031301(R) (2006).

[18] V. Y. Denisov, O. I. Davidovskaya, and I. Y. Sedykh, Phys. Rev. C **92**, 014602 (2015).

[19] J. G. Deng, J. C. Zhao, P. C. Chu, and X. H. Li, Phys. Rev. C **97**, 044322 (2018).

[20] D. Bai and Z. Ren, Phys. Rev. C **103**, 044316 (2021).

[21] D. Ni and Z. Ren, Phys. Rev. C **83**, 014310 (2011).

[22] Y. Qian, Z. Ren, and D. Ni, Phys. Rev. C **89**, 024318 (2014).

[23] D. N. Poenaru and R. A. Gherghescu, Phys. Rev. C **97**, 044621 (2018).

[24] D. S. Delion, Z. Ren, A. Dumitrescu, and D. Ni, J. Phys. G **45**, 053001 (2018).

[25] W. M. Seif and A. Abdurrahman, Chin. Phys. C **42**, 014106 (2018).

[26] D. Ni and Z. Ren, Phys. Rev. C **92**, 054322 (2015).

[27] Y. Qian and Z. Ren, J. Phys. G **43**, 065102 (2016).

[28] A. Bohr and B. Mottelson, *Nuclear Structure Vol. 2: Nuclear Deformations* (World Scientific, Singapore, 1998).

[29] G. Scamps, D. Lacroix, G. G. Adamian, and N. V. Antonenko, Phys. Rev. C **88**, 064327 (2013).

[30] G. I. Bykhalo, V. N. Orlin, and K. A. Stopani, arXiv:2107.08245 [nucl-th].

[31] Z. Wang, D. Bai, and Z. Ren, Phys. Rev. C **105**, 024327 (2022).

[32] W. M. Seif and A. Adel, Phys. Rev. C **99**, 044311 (2019).

[33] H. B. Yang, Z. G. Gan, Z. Y. Zhang, M. H. Huang *et al.*, Phys. Rev. C **105**, L051302 (2022).

[34] G. R. Satchler and W. G. Love, Phys. Rep. **55**, 183 (1979).

[35] D. T. Khoa, W. von Oertzen, and A. A. Ogloblin, Nucl. Phys. A **602**, 98 (1996).

[36] J. E. Perez Velasquez, N. G. Kelkar, and N. J. Upadhyay, Phys. Rev. C **99**, 024308 (2019).

[37] L. C. Chamon, B. V. Carlson, L. R. Gasques, D. Pereira, C. De Conti, M. A. G. Alvarez, M. S. Hussein, M. A. Candido Ribeiro, E. S. Rossi, Jr., and C. P. Silva, Phys. Rev. C **66**, 014610 (2002).

[38] C. N. Davids and H. Esbensen, Phys. Rev. C **61**, 054302 (2000).

[39] K. Wildermuth and Y. C. Tang, *A Unified Theory of the Nucleus* (Academic Press, New York, 1977).

[40] P. Möller, A. J. Sierk, T. Ichikawa, and H. Sagawa, At. Data Nucl. Data Tables **109–110**, 1 (2016).

[41] Y. Qian and Z. Ren, Phys. Rev. C **100**, 061302(R) (2019).

[42] W. J. Huang, M. Wang, F. G. Kondev, G. Audi, and S. Naimi, Chin. Phys. C **45**, 030002 (2021).

[43] M. Wang, W. J. Huang, F. G. Kondev, G. Audi, and S. Naimi, Chin. Phys. C **45**, 030003 (2021).

[44] F. G. Kondev, M. Wang, W. J. Huang, S. Naimi, and G. Audi, Chin. Phys. C **45**, 030001 (2021).

[45] P. Hornshøj, Nucl. Phys. A **230**, 365 (1974).

[46] Z. Y. Zhang, Z. G. Gan, L. Ma, L. Yu *et al.*, Phys. Rev. C **89**, 014308 (2014).

[47] A. K. Mistry, J. Khuyagbaatar, F. P. Heßberger, D. Ackermann *et al.*, Nucl. Phys. A **987**, 337 (2019).

[48] K. Eskola, P. Eskola, M. Nurmia, and A. Ghiorso, Phys. Rev. C **4**, 632 (1971).

[49] G. Audi and A. H. Wapstra, Nucl. Phys. A **595**, 409 (1995).

[50] Z. Wang, Z. Ren, and D. Bai, Phys. Rev. C **101**, 054310 (2020).

[51] C. Xu and Z. Ren, Phys. Rev. C **76**, 027303 (2007).

[52] Y. Qian and Z. Ren, Nucl. Phys. A **852**, 82 (2011).

[53] J. Zhang and H. F. Zhang, Phys. Rev. C **102**, 044308 (2020).

[54] J. P. Cui, Y. H. Gao, Y. Z. Wang, and J. Z. Gu, Nucl. Phys. A **1017**, 122341 (2022).

[55] T. Dong and Z. Ren, Phys. Rev. C **82**, 034320 (2010).

[56] B. M. Kayumov, O. K. Ganiev, A. K. Nasirov, and G. A. Yuldasheva, Phys. Rev. C **105**, 014618 (2022).